JOURNAL OF CATALYSIS **167,** 576–580 (1997)
ARTICLE NO. CA971593

NOTE

Redox Behavior of High Surface Area Rh-Loaded $Ce_{0.5}Zr_{0.5}O_2$ Mixed Oxide

Cerium oxide is widely employed as a promoter in the automotive three-way catalysts (TWCs) due to its high oxygen storage/release capacity (OSC). The OSC acts as an oxygen pressure regulator in the converter which allows one to maintain a high efficiency for the TWC (1). This has stimulated a strong interest in the investigation of redox properties of CeO_2-based catalysts (2). Recently, we disclosed that a $Ce_{0.5}Zr_{0.5}O_2$ mixed oxide with a surface area of 64 $m^2\ g^{-1}$ showed an unusual improvement of the redox behavior upon sintering induced by a repetitive reduction/oxidation of the solid solution (3, 4). In the present paper the redox behavior of the above Rh-loaded $Ce_{0.5}Zr_{0.5}O_2$ is reported. The influence of the thermal/redox treatment on the H_2 chemisorption is also addressed. Data obtained on a Rh/CeO_2 catalyst are included to elucidate the role of ZrO_2.

The $Ce_{0.5}Zr_{0.5}O_2$ solid solution was synthesized by a homogeneous gel route from $Ce(acac)_4$ and $Zr(O\text{-}Bu)_4$ precursors (Aldrich) according to a previous report (5). Briefly, the two precursors were refluxed in ethanol for 2 h, and then after evaporation of the solvent, the resulting gel was digested at 363 K for 2 days and finally dried at 393 K. The obtained solid was calcined at 773 K in air for 5 h. CeO_2 was kindly provided by Dr. L. Murrel. Metal impregnation was carried out by the incipient wetness method using a solution of $RhCl_3{\cdot}nH_2O$ to obtain a Rh nominal loading of 0.5 wt.%. The catalysts were dried at 393 K overnight and calcined at 773 K for 5 h. Henceforth, these samples are indicated as fresh ones.

Temperature programmed reduction (TPR) and oxygen uptake measurements were carried out as previously described (3). The oxidation was carried by a pulse technique at 700 K to ensure a full oxidation in the bulk of the solid solution (2). To minimize the contribution from adsorbed species to the TPR, all the samples were treated in Ar (20 ml min^{-1}) at 900 K for 5 h before the initial TPR experiment. N_2 adsorption isotherms at 77 K and H_2 chemisorption were carried out on a Micromeritics ASAP 2000 analyzer. The catalysts ($\approx$0.5 g) were reduced in a flow of H_2 (20 ml min^{-1}) at a heating rate of 10 K min^{-1} up to the selected reduction temperature. After 2 h at this temperature, they were degassed at 673 K for 5 h and cooled under vacuum to the adsorption temperature. Typically an equilibration time of 20 min was employed. The adsorbed volumes were determined by extrapolation to zero pressure of the linear part of the adsorption isotherm. FT-Raman spectra were performed on a Perkin Elmer 2000 FT-Raman spectrometer with a diode pumped YAG laser and a room temperature (RT) super InGaAs detector. The laser power was 50–200 mW. Powder X-ray diffraction patterns were collected on a Siemens 700 diffractometer using Ni-filtered Cu$K\alpha$.

Fresh $Ce_{0.5}Zr_{0.5}O_2$ features two peaks at 880 and 1010 K, respectively (Fig. 1, trace 1). The former peak is attributed to a reduction process occurring almost concurrently at the surface and in the bulk of the solid solution, while the latter one is associated with a process in the bulk (3). The sample was then oxidized at 700 K and recycled in further reduction/oxidation experiments. The reduction pattern is strongly affected as shown in trace 2 of Fig. 1. Remarkably, the reduction/oxidation treatments promote the reduction in the recycled $Ce_{0.5}Zr_{0.5}O_2$ since it is completed by 900 K.

Three peaks at 420, 620, and 1000 K are found for the fresh $Rh/Ce_{0.5}Zr_{0.5}O_2$ (Fig. 1, trace 3). The peak at 420 K is attributed to the reduction of the Rh_2O_3 precursor. A consumption of 0.023 mmol $H_2\ g^{-1}$ is measured for this peak which is lower than 0.073 mmol g^{-1} expected for the Rh_2O_3 reduction. The difference may be attributed to the presence of well dispersed Rh_2O_3 whose reduction may occur even at subambient temperatures. The presence of the supported Rh does not affect the peak at 1010 K, but it modifies that at 880 K as the temperature shifts to 620 K. A H_2 consumption of 0.68 mmol g^{-1} is measured for the peak at 620 K. $Rh/Ce_{0.5}Zr_{0.5}O_2$ features a surface area of 53 $m^2\ g^{-1}$ (Table 2) and therefore a H_2 consumption of 0.25 mmol g^{-1} is calculated upon application of the linear relationship between the surface area and H_2 consumption found by Perrichon *et al*. (6). Note that this is an upper limit for H_2 consumption since it is assumed that the surface contains only Ce^{4+} sites. Consequently, the peak at 620 K is attributed to reduction occurring both at the surface and in the bulk. After oxidation at 700 K, the sample was again subjected to TPR (Fig. 1, trace 4). All the reduction features at high temperatures disappear and a single peak at 440 K is observed. In all subsequent reduction/oxidation cycles, the TPR profile did not become modified further.

0021-9517/97 $25.00

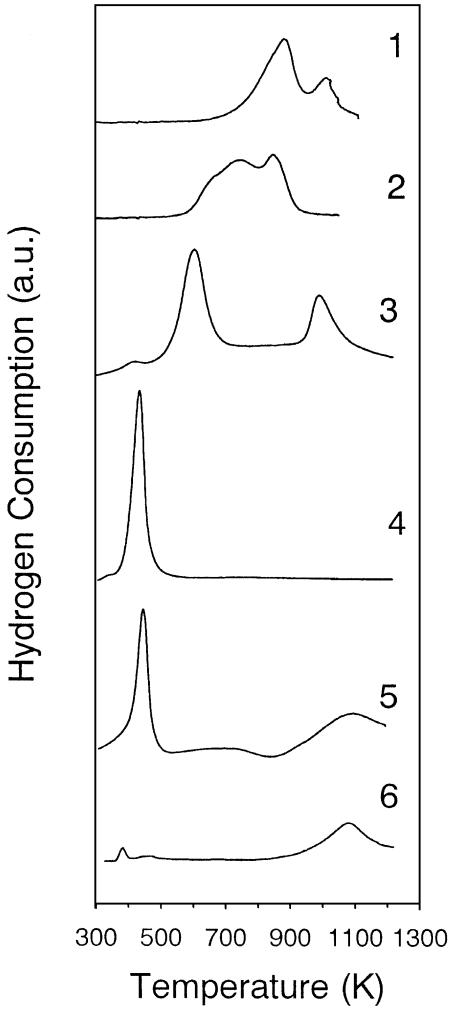

FIG. 1. Temperature programmed reduction of (**1**) fresh $Ce_{0.5}Zr_{0.5}O_2$, (**2**) $Ce_{0.5}Zr_{0.5}O_2$ seven-fold reduced/oxidized, (**3**) fresh $Rh/Ce_{0.5}Zr_{0.5}O_2$, (**4**) $Rh/Ce_{0.5}Zr_{0.5}O_2$ reduced/oxidized, (**5**) fresh Rh/CeO_2, (**6**) Rh/CeO_2 reduced/oxidized.

Comparison with Rh/CeO_2 is significant. Fresh Rh/CeO_2 (Fig. 1, trace 5) features strong reduction peaks at 440 and 1080 K. The peak at 440 K is associated with the rhodium precursor and CeO_2 surface reduction. The latter process is promoted by the supported metal. The peak at 1080 K is associated with the reduction of CeO_2 in the bulk (1). A perusal of the TPR profile reported in trace 5 of Fig. 1 reveals also a negative peak centered at about 850 K. Such negative peaks have been previously observed and attributed to desorption of H_2 and/or evolution of carbonates from the bulk of the support (6). After oxidation at 700 K, in the subsequent TPR only two minor peaks below 500 K are observed which can be attributed to the reduction of Rh_2O_3 with different particle sizes (2). The contribution of the support to the reduction at low temperatures is lost and the peak at 1080 K is the only relevant reduction feature remaining (Fig. 1, trace 6).

The oxygen uptakes at 700 K measured in the TPR/oxidation experiments are summarized in Table 1. Support reduction is associated with the formation of anionic oxygen vacancies in the solid solution due to the reducible Ce^{4+} cation. In Table 1, the degree of reduction is reported also as x in $Ce_mZr_{1-m}O_x$ ($m = 0.5$ or 1 is the Ce molar fraction), where $2 - x$ represents the total amount of oxygen vacancies formed by the reduction of the solid solution. Even though some reduction of surface Zr^{4+} cannot be excluded, it should only marginally affect the values of the Ce^{3+} reported in Table 1. Only a minor reduction was found for a Rh-loaded zirconia dispersed on SiO_2 below 1200 K (7) while no significant variation was detected in the XANES at the Zr K edge upon reduction of $Rh/Ce_{0.5}Zr_{0.5}O_2$ (8). Reduction of ZrO_2 in the bulk does not occur below 1200 K (2).

The degree of reduction of CeO_2 at 1273 K is independent of the sample history, e.g., fresh or recycled. A constant final composition of $CeO_{1.83}$ is obtained. By contrast, the ability to adsorb oxygen after a low temperature reduction is suppressed by the initial reduction of the CeO_2 up to 1273 K. This ability is present only in the fresh sample reduced at 700 K. The same behavior is observed for Rh/CeO_2. A partial oxidation of Rh^0 to Rh^{3+}, which easily occurs at 700 K, may account for the apparent higher formation of oxygen vacancies in the Rh/CeO_2 compared to CeO_2. Consistently, 0.036 mmol O_2 g^{-1} are calculated for the oxidation of Rh. Note that this amount is one order of magnitude smaller than the values reported in Table 1. For $Ce_{0.5}Zr_{0.5}O_2$, a small decrease of the oxygen uptake is observed during the first two runs but after the second recycle, a constant oxygen uptake is observed in all the subsequent

TABLE 1

O_2 Uptake Measured in the TPR/Oxidation Experiments Carried out on Metal-Free and Rh-Loaded $Ce_{0.5}Zr_{0.5}O_2$ and CeO_2

Sample	No. of recycles	O_2 uptake[a] (mmol g^{-1})	x in $Ce_mZr_{1-m}O_x$[b]	Ce^{3+} (%)[b]
$Ce_{0.5}Zr_{0.5}O_2$	0	0.53	1.84	62
	2–7	0.46	1.86	54
	8[c]	0.44	1.87	52
$Rh/Ce_{0.5}Zr_{0.5}O_2$	0	0.49	1.86	58
	1–3	0.53	1.85	64
	4[d]	0.43	1.88	50
CeO_2	0	0.50	1.83	35
	1–3	0.50	1.83	35
	4[c]	0.02	1.99	2
Rh/CeO_2	0	0.59	1.80	41
	1	0.58	1.81	40
	2[c]	0.02	1.99	2

[a] Measured after the TPR experiment carried out up to 1273 K, standard deviation ±0.01 mmol g^{-1}.

[b] Estimated from O_2 uptake, values not corrected for Rh oxidation.

[c] Isothermal reduction at 600 K for 2 h.

[d] Isothermal reduction at 440 K for 2 h.

experiments (Table 1). The redox process in $Ce_{0.5}Zr_{0.5}O_2$ is more efficient than in CeO_2 since about 50–60% of the cerium is reduced in the range 700–1273 K, giving a final composition of $Ce_{0.5}Zr_{0.5}O_{1.84-1.87}$. The presence of the supported Rh dose not affect significantly the ultimate value of the oxygen uptake since a composition of $Rh/Ce_{0.5}Zr_{0.5}O_{1.86}$ is obtained after the reduction at 1273 K. Noteworthy is the unusually high efficiency of the Ce^{3+}/Ce^{4+} redox couple in the recycled sample after a reduction at a temperature as low as 440 K (Table 1).

The influence of the thermal treatments on the textural properties was investigated by means of N_2 physisorption at 77 K. The results are reported in Table 2. Both fresh $Rh/Ce_{0.5}Zr_{0.5}O_2$ and Rh/CeO_2 show isotherms of type IV and H2 hysteresis according to the IUPAC classification which are indicative of the presence of a mesoporous texture. The isotherm of the fresh sample Rh/CeO_2 reveals a substantial contribution from micropores which is quite limited for the fresh $Rh/Ce_{0.5}Zr_{0.5}O_2$ (Table 2). The impregnation of $Ce_{0.5}Zr_{0.5}O_2$ with the $RhCl_3 \cdot nH_2O$ and subsequent calcination decrease the surface area from 64 to 53 $m^2\ g^{-1}$ which could be associated with some loss of microporosity upon calcination, even though the total pore volume is unaffected.

Upon thermal treatment at 900 K, there is a significant decrease of surface area which, in the case of Rh/CeO_2, is associated mainly with a loss of microporosity (9). Importantly, further reduction at 473 K, e.g., at surface reduction temperature, does not strongly decrease the surface area. A strong decrease of surface area is observed after reduction at 1000 K, e.g., at bulk reduction temperature. A similar behavior is observed for the $Rh/Ce_{0.5}Zr_{0.5}O_2$. Notably, the supported Rh interferes with the sintering of the support during the reduction at 1000 K (Table 2). The redox cycles destroy all the microporosity initially present while no significant decrease of pore volume due to mesopores is observed. The N_2 isotherms of the recycled Rh/CeO_2 and $Rh/Ce_{0.5}Zr_{0.5}O_2$ are still of type IV, but the hysteresis changes to type H3. This is an indication of an extensive pore restructuring. We calculate, according to Barrett *et al*. (BJH) (10), average pore diameters of 6.5 and 15 nm for Rh/CeO_2 and $Rh/Ce_{0.5}Zr_{0.5}O_2$, respectively. By contrast, the fresh samples show porosity only below 5 nm.

The parallel evolution of the texture of both Rh/CeO_2 and $Rh/Ce_{0.5}Zr_{0.5}O_2$ indicates that structural, rather than textural modifications are responsible for the different redox behavior. The modification of the cation sublattice and the metal–oxygen bonds of the $Rh/Ce_{0.5}Zr_{0.5}O_2$ upon redox cycles was investigated by XRD and Raman spectroscopy, respectively. XRD analysis (not reported) shows that the cation sublattice preserves the cubic Fm3m symmetry. The Raman spectra of fluorite-type oxides show a single band of T_{2g} symmetry which is located at 465 cm^{-1} for CeO_2. A strong broad band at 465 cm^{-1} was also observed in the Raman spectrum of $Ce_{0.5}Zr_{0.5}O_2$. Because of the width of the peak at 465 cm^{-1} and the presence of additional weak

TABLE 2

Textural Characterization of Metal-Free and Rh-Loaded CeO_2 and $Ce_{0.5}Zr_{0.5}O_2$ and of the Modifications Induced by *in Situ* Thermal and H_2 Treatments[a]

Sample	Treatment[b]			BET surface area ($m^2\ g^{-1}$)	Pore volume ($ml\ g^{-1}$)[c]			
						Mesopore	Micropore	
	T (K)	Gas	Time (h)		Total	V_{BJH}	V_t	V_{DR}
$Ce_{0.5}Zr_{0.5}O_2$	—	—	—	64	0.06	0.04	0.03	0.025
	1000	H_2	2	12	0.06	0.06	—	—
$Rh/Ce_{0.5}Zr_{0.5}O_2$	—	—	—	53	0.07	0.06	0.01	0.02
	900	N_2	5	30				
	473	H_2	2	29				
	1000	H_2	2	18	0.05	0.05	—	0.005
CeO_2	—	—	—	196	0.15	0.08	0.08	0.08
	1000	H_2	2	12	0.04	0.04	—	—
Rh/CeO_2	—	—	—	194	0.17	0.09	0.06	0.08
	900	N_2	5	164				
	473	H_2	2	154				
	1000	H_2	2	38	0.09	0.085	—	0.01

[a] All the samples were evacuated at 623 K to a constant pressure $\leq 2 \times 10^{-3}$ torr prior to N_2 adsorption.

[b] Treatment in flow of N_2 (20 ml min^{-1}), H_2 (20 ml min^{-1}), before N_2 adsorption, the reduced samples were oxidized at 700 K.

[c] Values determined from the adsorption isotherm by using: the BJH method in the range 3.5–170 nm; the *t* plot and the Dubinin–Radushkevich (DR) plot in the range 2×10^{-5}–0.1 p/p_0; total pore volume calculated at $p/p_0 = 0.98$ according to the Gurvitsch rule.

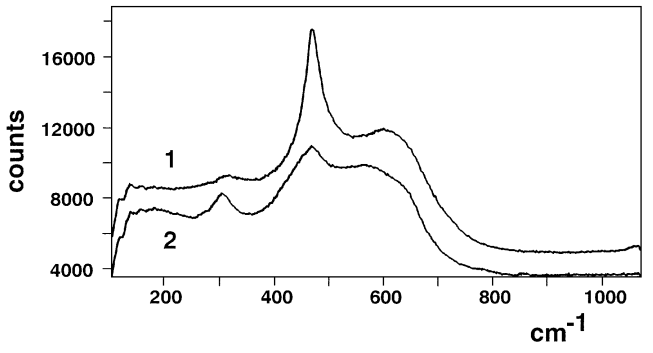

FIG. 2. Raman spectra of (**1**) fresh and (**2**) reduced at 1273 K/oxidized at 700 K $Rh/Ce_{0.5}Zr_{0.5}O_2$.

bands, this spectrum was attributed to a t'' phase (3) which is characterized by a cation sublattice of Fm3m symmetry and a tetragonal distortion of the oxygen sublattice (11). Fresh $Rh/Ce_{0.5}Zr_{0.5}O_2$ features a strong band centered at 465 cm^{-1}, a weak band at 313 cm^{-1}, and a broad band at about 620 cm^{-1} (Fig. 2, trace 1). This spectrum is similar to that of fresh $Ce_{0.5}Zr_{0.5}O_2$ except for the band at 620 cm^{-1} whose intensity is increased. A band at about 600 cm^{-1} was associated with oxygen vacancies created by substitution of Ce^{4+} in CeO_2-trivalent rare earth mixed oxides (12).

A strong decrease in the relative intensity of the band at 465 cm^{-1} is observed in the recycled $Rh/Ce_{0.5}Zr_{0.5}O_2$ (Fig. 2, trace 2). The same behavior was observed on $Ce_{0.5}Zr_{0.5}O_2$ reduced at 1000 K and then oxidized at 700 K, while reduction at 1273 K and oxidation at 700 K led to a complete disappearance of the band at 465 cm^{-1} (3).

This picture is consistent with an attribution of the improvement of the reduction at low temperatures to an increased displacement of the oxygen anions from the tetrahedral sites induced by thermal sintering of the $Ce_{0.5}Zr_{0.5}O_2$ in reducing conditions (3). The oxygen displacement favors a higher oxygen mobility in the bulk accounting for the modification of the redox behavior. Consistently, EXAFS characterization of a low surface area $Rh/Ce_{0.5}Zr_{0.5}O_2$ disclosed that the insertion of ZrO_2 into the CeO_2 modifies the oxygen sublattice (13). Some of the oxygens coordinated to the Zr^{4+} preserve the typical Zr–O distances, while two oxygens are pushed away from the Zr to a nonbonding distance longer than 0.28 nm. These two oxygens should be labile, accounting for the unusual promotion of the reduction in the bulk of the CeO_2–ZrO_2 solid solutions. Removal of two oxygens per Zr atom leads to a final stoichiometry of $Rh/Ce_{0.5}Zr_{0.5}O_{1.75}$. In fact, less oxygen vacancies are created in the reduction at 1273 K of $Rh/Ce_{0.5}Zr_{0.5}O_2$ (Table 1), suggesting that formation of a nonstoichiometric defective compound might limit the total degree of reduction.

The interaction with H_2 was studied by volumetric chemisorption after reduction at 473 and 1000 K (Table 3). Rh favors an extensive adsorption of hydrogen on CeO_2 due to a spillover phenomenon (14). On Rh/CeO_2 the H_2 spillover can be blocked by lowering the H_2 adsorption temperature which enables one to determine only the H_2 chemisorbed on the Rh particles (14). The apparent H/Rh ratios were measured at 233 and 308 K.

H/Rh = 0.86 is measured at 308 K over $Rh/Ce_{0.5}Zr_{0.5}O_2$ reduced at 473 K. After evacuation at 673 K, H/Rh decreases to 0.53, suggesting that the spillover is blocked to some extent; however, the H/Rh is still twice that measured at 233 K. Note that after a thermal treatment at 900 K, the same H/Rh ratio is measured at 233 and 308 K, which indicates that this treatment is able to block the spillover without inducing sintering of the metal particles. By contrast, the thermal treatment at 900 K does not eliminate the contribution of the spillover to the H_2 uptake in the case of Rh/CeO_2 as shown by the changes of H/Rh ratios with adsorption temperature (Table 3). Only after the reduction at 1000 K are equal H/Rh ratios measured on both the catalyst at 308 and 233 K.

The presence of ZrO_2 seems to be responsible for the easier suppression of the spillover in $Rh/Ce_{0.5}Zr_{0.5}O_2$ than in Rh/CeO_2. However, it could also be related to the stability of the surface area. After the thermal treatment at 900 K, there is a 45% and 15% drop of surface area, respectively, in the former and latter catalysts (Table 2). Changes in the rate of spilling of hydrogen over the support may account for the features of the TPR profiles. The suppression of the spillover by the initial thermal treatment at 900 K results in a shift of the reduction of the surface of $Ce_{0.5}Zr_{0.5}O_2$ to higher temperature compared to the reduction of Rh_2O_3. By contrast, the reduction of both the surface and Rh_2O_3 occur concurrently in Rh/CeO_2.

Reduction of Rh/CeO_2 at 773 K blocks H_2 spillover; however, upon oxidation and subsequent reduction at 623 K, the rate of H_2 spillover was recovered (14). After oxidation at

TABLE 3

Hydrogen Chemisorption on $Rh/Ce_{0.5}Zr_{0.5}O_2$ and Rh/CeO_2 Reduced at 473 and 1000 K

Catalyst	Reduction temperature (K)	H/Rh[a] (308 K)	H/Rh[a] (233 K)
$Rh/Ce_{0.5}Zr_{0.5}O_2$	473[b]	0.86	—
	473[c]	0.53	0.27
	473[d]	0.27	0.27
	1000	0.21	0.20
Rh/CeO_2	473[d]	0.80	0.21
	1000[d]	0.14	0.15

[a] Hydrogen chemisorption measured at the indicated temperature.
[b] Fresh sample.
[c] Sample degassed *in vacuo* at 673 K for 5 h before reduction.
[d] Sample pretreated in N_2 at 900 K for 5 h before reduction.

700 K, the peak at 620 K is shifted to 440 K in the TPR profile of the recycled $Rh/Ce_{0.5}Zr_{0.5}O_2$, which suggests that an efficient H_2 activation occurs. The increase in the efficiency of H_2 activation cannot by itself account for the modification of the TPR profile of the recycled Rh-loaded sample. The lack of observation of the peak at 1000 K is consistent with the results observed over the unsupported sample (Fig. 1, trace 2) and is associated with the promoting effects of sintering on the redox properties of the $Ce_{0.5}Zr_{0.5}O_2$ solid solution. The TPR profile of a low surface area ($\approx 1\ m^2\ g^{-1}$) cubic $Rh/Ce_{0.5}Zr_{0.5}O_2$ solid solution showed two peaks attributable to the reduction of the support in the bulk which was attributed to clustering of oxygen vacancies during the reduction (2). At variance with this, the TPR of the recycled Rh-loaded $Ce_{0.5}Zr_{0.5}O_2$ shows a single reduction feature (Fig. 1, trace 4), suggesting that the role of the supported metal is not limited to a simple activation of H_2. Upon reduction of the fresh sample, the surface area strongly decreases due to pore-filling and support sintering (3). Such a process would easily lead to an encapsulation of part of the metal particles decreasing the H/Rh from 0.27 to 0.20, as observed after reduction at 473 and 1000 K, respectively, even though a partial sintering of Rh particles cannot be excluded.

A model for the reduction process of fluorite oxides invokes filling of oxygen vacancies by transition metal atoms (15). Such a process could easily interfere with the clustering of oxygen vacancies, thus accounting for the single reduction peak in the recycled $Rh/Ce_{0.5}Zr_{0.5}O_2$. In addition, Rh promotes the oxygen migration from the bulk of CeO_2 to the surface of the metal particles (16). Further work is necessary to elucidate the role of the metal in the kinetics of the reduction process. The above model (15) can also be invoked for the stabilization of the surface area in the presence of the supported metal. As shown by SEM investigation of the $Ce_{0.5}Zr_{0.5}O_2$ (3), the redox cycles induce a strong sintering of the support via a surface diffusion and/or vapor transport. Such processes can be suggested also for the sintering of the present Rh-loaded samples since they smooth the initial surface roughness without inducing pore shrinkage. Accordingly the decrease of the surface area leaves the mesopore volume unaffected.

ACKNOWLEDGMENTS

Prof. Adriano Bigotto, Dr. Roberta Di Monte (University of Trieste), and Dr. Elena Bekaryova (Bulgarian Academy of Sciences, Sofia) are acknowledged for helpful discussions. MURST 40%, CNR (Rome), and University of Trieste are acknowledged for financial support.

REFERENCES

1. Taylor, K. C., *Catal. Rev. Sci. Eng.* **35**, 457 (1993); Harrison, B., Diwell, A. F., and Hallett, C., *Plat. Met. Rev.* **32**, 73 (1988); Yao, H. C., and Yu Yao, Y. F., *J. Catal.* **87**, 152 (1984).
2. Fornasiero, P., Di Monte, R., Ranga Rao, G., Kašpar, J., Meriani, S., Trovarelli, A., and Graziani, M., *J. Catal.* **151**, 168 (1995).
3. Fornasiero, P., Balducci, G., Di Monte, R., Kašpar, J., Sergo, V., Gubitosa, G., Ferrero, A., and Graziani, M., *J. Catal.* **164**, 173 (1996).
4. Balducci, G., Fornasiero, P., Di Monte, R., Kašpar, J., Meriani, S., and Graziani, M., *Catal. Lett.* **33**, 193 (1995).
5. Meriani, S., and Soraru, G., "Ceramic Powders" (P. Vicenzini, Ed.), p. 547. Amsterdam, Elsevier, 1983.
6. Perrichon, V., Laachir, A., Bergeret, G., Fréty, R., Tournayan, L., and Touret, O., *J. Chem. Soc. Faraday Trans.* **90**, 773 (1994).
7. Borer, A. L., Bronnimann, C., and Prins, R., *J. Catal.* **145**, 516 (1994).
8. Ranga Rao, G., Fornasiero, P., Di Monte, R., Kašpar, J., Vlaic, G., Balducci, G., Meriani, S., Gubitosa, G., Cremona, A., and Graziani, M., *J. Catal.* **162**, 1 (1996).
9. Perrichon, V., Laachir, A., Abouarnadasse, S., Touret, O., and Blanchard, G., *Appl. Catal. A Gen.* **129**, 69 (1995).
10. Barrett, E. P., Joyner, L. G., and Halenda, P. P., *J. Am. Chem. Soc.* **73**, 373 (1951).
11. Yashima, M., Arashi, H., Kakihana, M., and Yoshimura, M., *J. Am. Ceram. Soc.* **77**, 1067 (1994).
12. McBride, J. R., Hass, K. C., Poindexter, B. D., and Weber, W. H., *J. Appl. Phys.* **76**, 2435 (1994).
13. Vlaic, G., Kašpar, J., Geremia, S., Fornasiero, P., and Graziani, M., *J. Catal.*, accepted for publication (1997).
14. Bernal, S., Botana, F. J., Calvino, J. J., Cauqui, M. A., Cifredo, G. A., Jobacho, A., Pintado, J. M., and Rodriguez-Izquierdo, J. M., *J. Phys. Chem.* **97**, 4118 (1993); Bernal, S., Calvino, J. J., Cifredo, G. A., Laachir, A., Perrichon, V., and Herrmann, J. M., *Langmuir* **10**, 717 (1994).
15. Sanchez, M. G., and Gazquez, J. L., *J. Catal.* **104**, 120 (1987).
16. Cordatos, H., Bunluesin, T., Stubenrauch, J., Vohs, J. M., and Gorte, R. J., *J. Phys. Chem.* **100**, 785 (1996).

P. Fornasiero
J. Kašpar[1]
M. Graziani

Dipartimento di Scienze Chimiche
Università di Trieste
Via Giorgieri 1
34127 Trieste, Italy

Received April 18, 1996; revised September 30, 1996; accepted December 13, 1996

[1] To whom correspondence should be addressed. Fax: ++39-40-6763903. E-mail: kaspar@dschsun1.univ.trieste.it.